Separation Science and Technology
Publication details, including instructions for authors and subscription information:
http://www.informaworld.com/smpp/title~content=t713708471

Retention of Paramagnetic Particles by Magnetite Particle Clusters with Multifunctional Character

Armin D. Ebner[a]; James A. Ritter[a]
[a] Department of Chemical Engineering, Swearingen Engineering Center, University of South Carolina, Columbia, South Carolina, USA

Online publication date: 08 July 2010

To cite this Article Ebner, Armin D. and Ritter, James A.(2004) 'Retention of Paramagnetic Particles by Magnetite Particle Clusters with Multifunctional Character', Separation Science and Technology, 39: 12, 2785 — 2808
To link to this Article: DOI: 10.1081/SS-200028807
URL: http://dx.doi.org/10.1081/SS-200028807

SEPARATION SCIENCE AND TECHNOLOGY
Vol. 39, No. 12, pp. 2785–2808, 2004

Retention of Paramagnetic Particles by Magnetite Particle Clusters with Multifunctional Character

Armin D. Ebner and James A. Ritter*

Department of Chemical Engineering, Swearingen Engineering Center, University of South Carolina, Columbia, South Carolina, USA

ABSTRACT

The magnetic force exerted by a 3-D array of five hundred identical magnetite particles (with $r_m = 400$ nm) on two differently sized paramagnetic particles (with $r_p = 160$ and 1000 nm) was investigated to reveal the multifunctional character of magnetic particle clusters that may prove to be advantageous when used as a HGMS element. The orientation of the magnetic field, the separation s between the magnetite particles in the array, and the distance h between the paramagnetic particle and the surface of the magnetite array were all found to have significant effects. Both the large and small paramagnetic particles experienced interactions with the array that were strictly due to the array behaving collectively as a single magnetic unit; but these relatively "smooth" interactions were

*Correspondence: James A. Ritter, Department of Chemical Engineering, Swearingen Engineering Center, University of South Carolina, Columbia, SC 29208, USA; Phone: (803) 777-3590; Fax: (803) 777-8265; E-mail: ritter@engr.sc.edu.

DOI: 10.1081/SS-200028807 0149-6395 (Print); 1520-5754 (Online)

much longer-ranged for the large paramagnetic particle. The large and small paramagnetic particles also experienced interactions with the array that were strictly due to individual (yet cooperative) interactions with each of the magnetite particles in the array; but in most cases these individual and relatively "rough" interactions were short-ranged for both paramagnetic particles. The spatial range of these solitary (multifunctional) interactions depended markedly on the values of h and s, and especially r_p, as did the regions where these collective and individual interactions overlapped. The orientation of the magnetic field produced maximum and bounding interactions when $\alpha = 0^\circ$ and $\alpha = 90^\circ$, with the resulting repulsive interactions at $\alpha = 0^\circ$ (with H_a parallel to the surface of the array) always being less than the resulting attractive interactions at $\alpha = 90^\circ$ (with H_a perpendicular). As a HGMS element, this unique multifunctional character of magnetite particle clusters could give various forms of supported magnetite a key advantage over traditional stainless steel wool for retaining both large and especially small paramagnetic particles of weak magnetic character.

Key Words: Magnetic forces; High gradient magnetic separation; Magnetite particles; Magnetite clusters; Paramagnetic particles.

INTRODUCTION

In recent years, researchers[1–5] have been exploring the possibility of using magnetite as a magnetically energizable element in high-gradient magnetic separation (HGMS) processes. This interest stems from magnetite having a relatively large saturation magnetization and a naturally occurring size that is much smaller than traditional stainless steel wool. These properties, in turn, give magnetite the potential to be a more effective magnetic element than stainless steel wool for removing relatively small paramagnetic particles. Experimental attempts in using magnetite as a HGMS element were initially carried out by Kochen et al.,[1] wherein a polyimeric resin coated with magnetite was developed and successfully tested for the removal of actinide species from alkaline radioactive wastes. Shortly thereafter, by theoretically analyzing the feasibility and limitations of the retention ability of magnetite in a HGMS process, Ebner et al.[2–4] provided considerable insight into the relative roles played by magnetic and other forces that naturally occur between a single magnetite particle and a paramagnetic particle, including Brownian, van der Waals, and electrostatic forces.

More recently, Ebner et al.[5] explored the effect imparted by the magnetic interaction between a paramagnetic particle and a magnetite particle when being exposed to a cluster of neighboring magnetite particles of identical size.

This study showed the particularly significant effect the separation between the magnetite particles in the array had on both smoothing the individual interactions between the magnetite particle and the paramagnetic particle, and on creating zones between the adjacent magnetite particles where the paramagnetic particle experiences both attractive and repulsive interactions at any orientation of the magnetic field and when in close proximity to the array. They[5] also found a weak magnetic interaction that persisted at much greater distances between the array and the paramagnetic particle than ever exhibited by an individual magnetite particle and the paramagnetic particle. Because these longer-ranged interactions became more pronounced at closer separations between the magnetite particles in the array, they were attributed to the entire array behaving as a single magnetic unit. This intriguing result was of paramount importance because it revealed a unique multifunctional magnetic character of magnetite arrays manifested by the ability of the array to remove paramagnetic particles not only of sizes comparable to an individual magnetite particle, but also of sizes comparable to the entire array itself. In other words, this multifunctional magnetic character allows magnetite to remove paramagnetic particles ranging in sizes from very small ones that can be removed only by magnetic elements the size of an individual magnetite particle to very large ones the size of which depends on the size of the magnetite array.

Since the previous study[5] only considered the retention of small paramagnetic particles on the order of the size of an individual magnetite particle, the objective of this study is to reveal the effect of the magnetite array on retaining very large paramagnetic particles on the order of the size of the array. Hence, paramagnetic particles with radii of 160 and 1000 nm are studied to explore the subtle transition between the short-ranged magnetic forces associated with the individual magnetite particles in the array and the long-ranged magnetic forces associated with the entire array of magnetite particles behaving as a single magnetic unit, for both relatively small and relatively large paramagnetic particles. Three key variables that affect the net magnetic force on the paramagnetic particle are studied: the orientation of the magnetic field, the distance between the magnetite particles in the array, and the normal distance between the paramagnetic particle and the array. Other parameters, such as the magnetic field strength, the size of the magnetite particle in the array, and the size of the array are held constant in this theoretical analysis to clearly reveal the multifunctional behavior of a magnetite cluster.

MODEL DEVELOPMENT

Figure 1a shows the same magnetite array utilized in the earlier work[5] that consists of a $10 \times 10 \times 5$ block of equally sized magnetite particles of

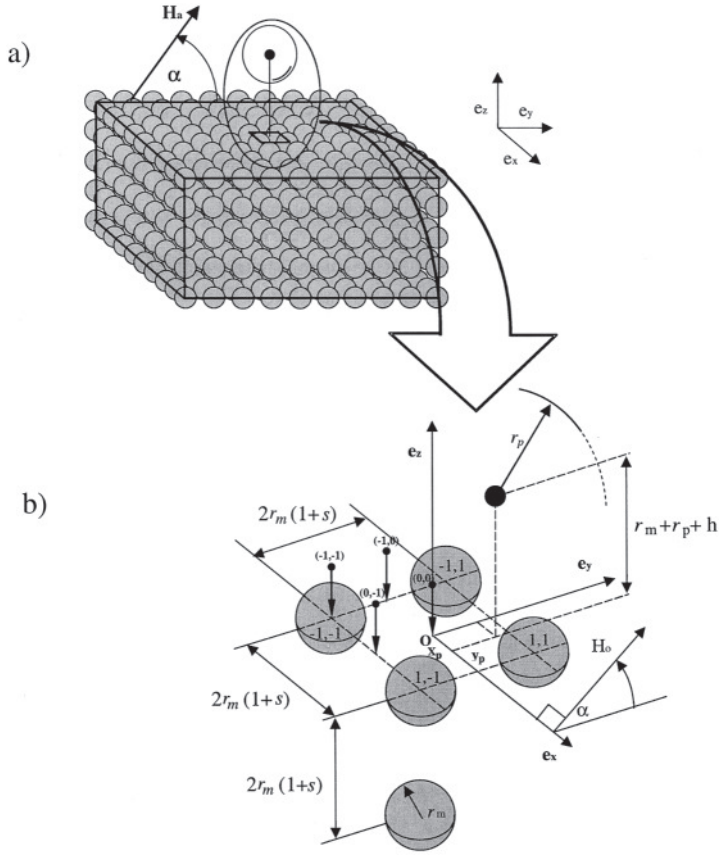

Figure 1. Schematic of (a) the three-dimensional array containing 10 × 10 × 5 magnetite particles and a paramagnetic particle and (b) close-up of the central rectangular region in the x–y plane at the surface of the array where the magnetic interactions are calculated.

radius r_m. In this case, however, the paramagnetic particle of radius r_p that is centrally located at some distance above the top layer of the magnetite particle array is either considerably larger or about the same size as a single magnetite particle. As before, the separation between each magnetite particle in the array is the same, and the entire array is subjected to a magnetic field H_a inclined at angle α with respect to the y-axis and lying parallel to the z-y plane. An augmented view of the x-y plane, within which the interactions between the array of magnetite particles and the paramagnetic particle are calculated, is shown in Figure 1b. The region defined in the x–y plane consists of a square of area

$2r_m(1+s) \times 2r_m(1+s)$ bounded by the centers of the four innermost magnetite particles of the top layer, where the parameter s is the ratio between the surface-to-surface separation between the magnetite particles and their diameter. The paramagnetic particle is placed at a distance $r_m + r_p + h$ above the array, where h represents the surface-to-surface distance between the paramagnetic particle and the plane that is tangent to the top layer of the magnetite particles in the array and parallel to the x-y plane. With the origin defined at the center of the square, the Z_p coordinate of the paramagnetic particle is given by

$$Z_p = r_m + r_p + h \tag{1a}$$

with the X_p^* and Y_p^* coordinates restricted to the following limits

$$-r_m(1+s) \le X_p \le r_m(1+s) \tag{1b}$$

$$-r_m(1+s) \le Y_p \le r_m(1+s) \tag{1c}$$

For magnetite particle i in the array, the coordinates are defined as

$$X_{m,i} = (-9 + 2(k_i - 1))^* r_m(1+s) \qquad k_i = 1, 2, \ldots, 10 \tag{2a}$$

$$Y_{m,i} = (-9 + 2(l_i - 1))^* r_m(1+s) \qquad l_i = 1, 2, \ldots, 10 \tag{2b}$$

$$Z_{m,i} = (-2(m_i - 1))^* r_m(1+s) \qquad m_i = 1, 2, \ldots, 5 \tag{2c}$$

The derivation of the expressions that describe the net force on a single paramagnetic particle due to the 3-D array of magnetite particles is simplified through the application of the superposition property of magnetic fields.[5,7–10] To analyze the magnetic force over a paramagnetic particle of any arbitrary size, the following exact analytical expressions developed by Eisenstein[6] in spherical coordinates for the components of the magnetic force exerted by a single magnetite particle on a paramagnetic particle of a given size are utilized:

$$\begin{aligned} F_{m,r} = V_p \mu_o (\chi_p - \chi_m) \cdot \Bigg[& -\frac{3H_a G}{r^4}(3\cos^2\theta - 1) - \frac{9G^2 r}{2(r^2 - r_p^2)^4}(\cos^2\theta + 1) \\ & + \frac{3G^2(3r_p^4 - 3r^4 - 8r^2 r_p^2)}{32 r_p^2 r^3 (r^2 - r_p^2)^3}(3\cos^2\theta - 1) \\ & + \frac{9G^2}{64 r_p^3 r^4} \ln\left(\frac{r + r_p}{r - r_p}\right)(3\cos^2\theta - 1) \Bigg] \end{aligned} \tag{3a}$$

$$\begin{aligned} F_{m,\theta} = V_p \mu_o (\chi_p - \chi_m) \cdot \Bigg[& -\frac{3H_a G}{r^4} - \frac{3G^2}{4r(r^2 - r_p^2)^3} - \frac{9G^2(r_p^2 + r^2)}{32 r_p^2 r^3 (r^2 - r_p^2)^2} \\ & + \frac{9G^2}{64 r_p^3 r^4} \ln\left(\frac{r + r_p}{r - r_p}\right) \Bigg] \sin^2\theta \end{aligned} \tag{3b}$$

θ is the angle formed by the line containing the center of the magnetite particle and parallel to the applied field H_a, and the lines of centers of the paramagnetic particle and the magnetite particles. The center-to-center distance between these two particles is r. M_s is the magnetization of the magnetite particle, which is assumed to be at saturation; V_p is the volume of the paramagnetic particle; χ_p and χ_m are the volumetric susceptibilities of the magnetic particle and the medium, respectively. G is a constant and proportional to the magnetic moment μ_m of the spherical magnetite particle according to

$$G = \frac{\mu_m}{4\pi} = \frac{M_s r_m^3}{3} \tag{3c}$$

However, since the expressions given in Eq. (3) are in spherical coordinates, they are origin-dependent and cannot be used directly to calculate the net force exerted by the array on the paramagnetic particle. This problem is resolved if each of the magnetite-paramagnetic particle interactions defined according to the spherical coordinate system of Eq. (3) are transformed into the common Cartesian coordinate system presented in Fig. 1. In this way, the superposition principle can be used to sum directly the components of all the individual pair interactions. After this transformation, the net magnetic force is given by

$$F_{m,j} = \sum_{i=1}^{N} F_{m,i,j}, \qquad j = x, y \text{ or } z \tag{4}$$

where $F_{m,i,j}$ represents the component of the magnetic force due to magnetite particle i interacting with the paramagnetic particle along direction j (i.e., $j = x$, y or z) with N being the total number of magnetite particles in the system. It has been shown previously[5] that the components of the force can be determined by carrying out the following transformations:

$$\begin{bmatrix} F_{m,i,x} \\ F_{m,i,y} \\ F_{m,i,z} \end{bmatrix}^T = \begin{bmatrix} F_{m,i,x'} \\ F_{m,i,y'} \\ F_{m,i,z'} \end{bmatrix}^T \begin{bmatrix} 1 & 0 & 0 \\ 0 & \sin\alpha & -\cos\alpha \\ 0 & \cos\alpha & \sin\alpha \end{bmatrix} \tag{5}$$

$$\begin{bmatrix} F_{m,i,x'} \\ F_{m,i,y'} \\ F_{m,i,z'} \end{bmatrix}^T = \begin{bmatrix} F_{m,i,r} \\ F_{m,i,\theta} \\ 0 \end{bmatrix}^T \begin{bmatrix} \sin\theta_i\cos\phi_i & \sin\theta_i\sin\phi_i & \cos\theta_i \\ \cos\theta_i\cos\phi_i & \cos\theta_i\sin\phi_i & -\sin\theta_i \\ -\sin\phi_i & \cos\phi_i & 0 \end{bmatrix} \tag{6}$$

where $F_{m,i,r}$ and $F_{m,i,\theta}$ are given by Eqs. (3a) and (3b) for spherical coordinates r_i and θ_i of a given magnetite particle *i*. The trigonometric functions of these coordinates are given by:

$$\cos\theta_i = \frac{\overline{AB}}{r_i} = \frac{Z_i^* \sin\alpha + Y_i^* \cos\alpha}{r_i} \tag{7}$$

$$\sin\theta_i = \sqrt{1 - \cos^2\theta_i} \tag{8}$$

$$\cos\phi_i = \frac{\overline{OD}}{\overline{AO}} = \frac{X_i^*}{r_i \sin\theta_i} \tag{9}$$

$$\sin\phi_i = \frac{\overline{AD}}{\overline{AO}} = -\frac{Z_i^* \cos\alpha - Y_i^* \sin\alpha}{r_i \sin\theta_i} \tag{10}$$

with

$$r_i = (X_i^{*2} + Y_i^{*2} + Z_i^{*2})^{0.5} \tag{11}$$

and X_i^*, Y_i^*, and Z_i^* being the cartesian coordinates of the particle with respect to magnetite particle *i*, i.e.,

$$X_i^* = X_p - X_{m,i} \tag{12a}$$

$$Y_i^* = Y_p - Y_{m,i} \tag{12b}$$

$$Z_i^* = Z_p - Z_{m,i} \tag{12c}$$

Note that the expression presented in Eq. (10) for evaluating $\sin\phi_i$ is preferred over the traditional trigonometric identity $\sin\phi_i = \sqrt{1 - \cos^2\phi_i}$ to cope with the sign problems that arise from the symmetry of the above vectorial transformations. A detailed explanation of the methodology applied to solve the above system of equations and transformations is given elsewhere.[5]

RESULTS AND DISCUSSION

As done in previous studies,[2–4,10] the forces here are evaluated in dimensionless form relative to the Brownian force by dividing their magnitude by $|k_bT/r_p|$, i.e.,

$$F_{m,j}^* = \left|\frac{r_p}{kT}\right| F_{m,j} \tag{13}$$

When the magnitude of this dimensionless expression is $\gg 1$, the force on the paramagnetic particle is strong enough to overcome any thermal motion, and an absolute value >10 is considered to be strong enough to dominate the randomizing effect of Brownian motion. Table 1 lists the values and ranges

Table 1. Model parameters and ranges.

α	0; 90°
s	0.0–1.0
h (nm)	20–1000
H_a (A m^{-1})	2,387,319
M_s (A m^{-1})	480,000
r_p (nm)	160; 1000
r_m (nm)	400
χ_p	250×10^{-6}
χ_m	13×10^{-6}

of the parameters utilized in the model. Four main variables are considered: the angle α, the distance h between the paramagnetic particle and the array, the dimensionless half surface-to-surface separation s between the magnetite particles (which is defined in terms of the magnetite particle radius), and the variables x and y, which represent the dimensionless x and y coordinates of the paramagnetic particle with the origin of these coordinates positioned as depicted in Fig. 1b, i.e.,

$$x = \frac{X_p}{r_m(1+s)} \tag{14a}$$

$$y = \frac{Y_p}{r_m(1+s)} \tag{14b}$$

All the other parameters are kept constant. For simplicity, the four magnetite particles closest to the paramagnetic particle are referred to the location of their centers according to the dimensionless x and y coordinates, again as shown in Fig. 1b. Also, it is worth pointing out that the value chosen for the volumetric magnetic susceptibility of the paramagnetic particle ($\chi_p = 250 \times 10^{-6}$) corresponds to a weekly paramagnetic species like CuO or PuO_2.

Figure 2 shows the effect of the distance h between the paramagnetic particle and the surface of the array on the z-component of the total force on the paramagnetic particle with a 1000 nm radius at different separations between the magnetite particles (i.e., $s = 1.0$, 0.4, and 0.0), and for two different orientations of the applied magnetic field (i.e., $\alpha = 0$ and 90°). The z-component of the force is evaluated at four fixed dimensionless x and y coordinates of the paramagnetic particle, i.e., (0,0), (−1,0), (0, −1), and (−1, −1) (as indicated by the vertical arrows in Fig. 1b). The z-component of the force on the paramagnetic particle by a single magnetite particle at (−1, −1) is also shown. As discussed in the previous work,[10] several important conclusions can be

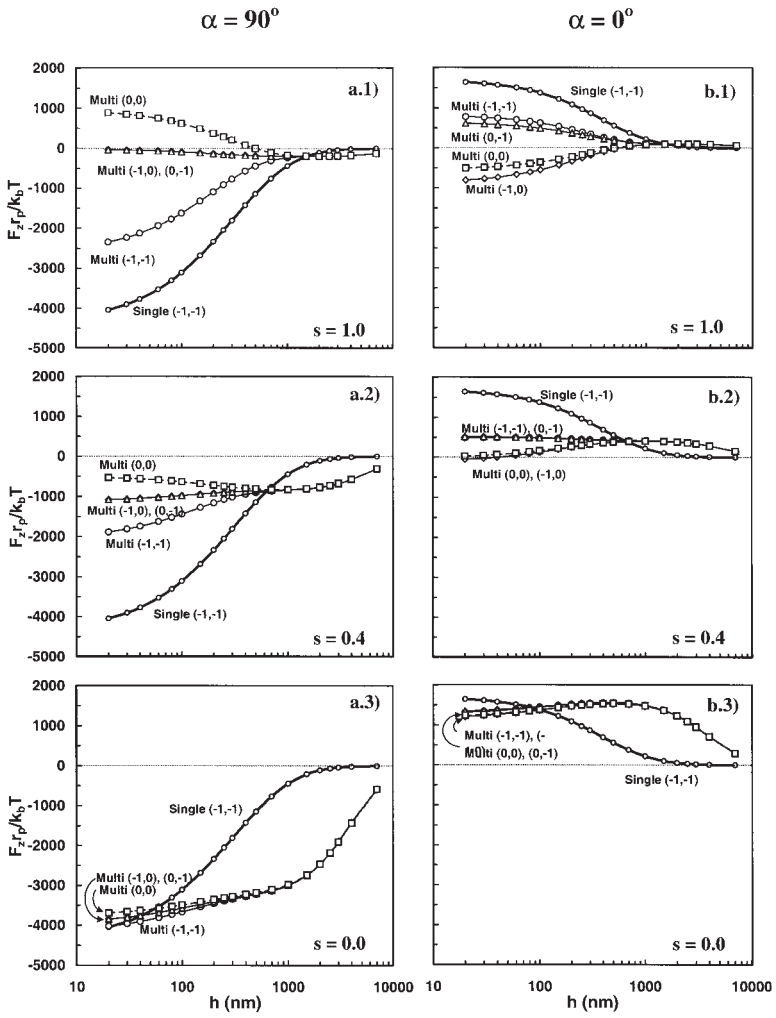

Figure 2. z-Component of the total magnetic force exerted by the array of magnetite particles on the paramagnetic particle with radius r_p equal to 1000 nm as a function of the distance h between the paramagnetic particle and the array at different locations within the square defined in Fig. 1b for magnetic field orientation α equal to a) 90° and b) 0°, and for separation s between the magnetite particles of 1) 1.0, 2) 0.4, and 3) 0.0. All other parameters are fixed and given in Table 1. "Single" stands for a single magnetite particle interacting with a paramagnetic particle, and "multi" stands for multiple magnetite particles interacting with a paramagnetic particle.

gleaned from the results shown in Fig. 2. First, in general, at very close distances between the array and the paramagnetic particle (i.e., small h) the interaction felt by the paramagnetic particle is dominated by the individual interactions between this particle and the magnetite particles in the array. Moreover, the net force exerted on the paramagnetic particle by the array is never larger than the interaction between a single magnetite particle and the paramagnetic particle just in front of it, which is denoted by the thick lines labeled single in Fig. 2. This interesting behavior results from the opposing lateral interactions experienced by the paramagnetic particle as it approaches the surface of the array (decreasing h). In effect, at closer distances to the array, the paramagnetic particle becomes more laterally surrounded by magnetite particles, wherein the sum of each of the individual interactions between the paramagnetic particle and the neighboring magnetite particles sum up destructively. This effect becomes more pronounced with larger magnetite particle separations (i.e, increasing s), even to the point where the force changes sign. For example, in Fig. 2a.3 (where $s = 0.0$ and $\alpha = 90^\circ$) the force on the paramagnetic particle at (0,0) is attractive (negative) for all h; but, as the separation between the magnetite particles increases from $s = 0.0$ to $s = 1.0$, the interaction changes sign and becomes repulsive for $h < 600$ nm (Fig. 2a.1). For identical reasons, when the applied magnetic field is parallel to the surface of the array (i.e., with $\alpha = 0$), as shown in Figs. 2b.3 to 2b.1, the opposite behavior is observed, but with about half the magnitude of the interaction force. For magnetic particle clusters with randomly distributed surfaces, on average, α is expected to be about 45°, which suggests that the magnitude and direction (i.e., attractive or repulsive) of the interaction force is essentially bounded by the orthogonal orientation of the magnetic field at $\alpha = 0$ and 90°.

Another feature observed in Fig. 2 is that for relatively close distances h between the paramagnetic particle and the array, the strongest interactions between the array and the paramagnetic particle always occur when the paramagnetic particle is centrally aligned with a magnetite particle in the array [e.g., at location $(-1, -1)$]. Note that the forces associated with the central locations of the other three magnetite particles depicted in Fig. 1b [i.e., locations $(-1,1)$, $(1, -1)$ and $(1,1)$], but not shown in Fig. 2, would be essentially identical to those at location $(-1, -1)$ due to symmetry and while ignoring minor edge effects. At the other noncentral locations depicted in Fig. 1b, like (0,0), $(-1,0)$, and $(0, -1)$, the forces are necessarily less, as shown in Fig. 2. This result is due to the closer proximity of the paramagnetic particle to neighboring magnetite particles, where (as pointed out) the individual interactions between the paramagnetic particle and the neighboring magnetite particles sum up destructively, especially at small values of h. Again, these strongest or maximum interactions occur only when the field is

exactly perpendicular ($\alpha = 90^\circ$) or parallel to the surface ($\alpha = 0^\circ$), with the interaction being attractive or repulsive, respectively. At all other magnetic field orientations α, the interactions would necessarily be somewhere in between and hence less than those observed in Fig. 2.

Also notice that in all cases depicted in Fig. 2, as the distance between the array and the paramagnetic particle increases (i.e., increasing h), all the spatially-dependent short-ranged interactions merge into one long-ranged interaction at about $h = 600$ nm that slowly decays as h increases to 10 μm. Upon comparing the magnetite particle cluster results with the single magnetite particle results, it becomes clear that the interactions observed for $h < 600$ nm (for this particular large paramagnetic particle system) are due to short-ranged interactions caused by the individual interaction between the paramagnetic particle and the nearby magnetite particles. This fact becomes even more apparent as the separation s between the magnetite particles increases, because the departure from the single magnetite particle results becomes more pronounced for either magnetic field orientation α. In contrast, the interactions observed for $h > 600$ nm that do not depend on the x and y coordinate can be explained only by the array behaving as a single magnetite unit. This fact becomes very apparent as the separation s between the magnetite particles decreases, wherein the long-ranged forces become much more pronounced with significant departure from the single magnetite particle results, again for either magnetic field orientation α. In other words, for $h > 600$ nm (in this case) and $s = 1.0$, the force exerted on the large paramagnetic particle by multiple magnetite particles is no greater than that exerted by a single magnetite particle (Figs. 2a.1 and 2b.1); however, for $h > 600$ nm and $s = 0.0$, the force imparted to the large paramagnetic particle by multiple magnetite particles is far greater that that imparted by a single magnetite particle (Figs. 2a.3 and 2b.3), clearly indicating the long-ranged and "collective" effects of the array behaving as a single magnetite unit. It is clear then that the influence of the array as a single magnetic unit becomes stronger when the magnetite particles become closer to each other (i.e., smaller s). This behavior is simply due to the fact that the effective magnetization of the array naturally increases when there is less space between the magnetite particles (decreasing s), which in turn causes the array to behave more and more like one large magnetic unit.

Another surprising characteristic of the array is that in some instances the net force exerted by it on the paramagnetic particle not only exhibits a maximum (whether attractive or repulsive) with decreasing h, as exhibited by numerous curves in Fig. 2, but it also changes sign (i.e., from being attractive to repulsive or vice versa) with decreasing h, as exhibited by the curves corresponding to the location (0,0) for $s = 1.0$ in Figs. 2a.1 or 2b.1. These intriguing results are simply a consequence of the short- and long-ranged

interactions becoming coupled with each other. For example, as shown in Fig. 2a, the short-ranged interactions caused by the individual magnetite particles are repulsive, while the long-ranged interactions caused by the array of magnetite particles behaving as a single magnetic unit are attractive. In this situation, it is surmized that the large paramagnetic particle would follow a rather unique trajectory as it approaches the array and experiences these two types of interactions. First, if attracted by strong enough long-ranged interactions due to the cooperative effect of the array as a whole, it would begin approaching the array toward those regions where the long-ranged interactions remain attractive. At a given proximity to the array, however, this paramagnetic particle would begin to feel the short-ranged interactions due to individual interactions with each of the magnetite particles at or near the surface of the array. At this point, the paramagnetic particle would sense a sort of "roughness" and selectively move only toward regions with strong and attractive short-ranged interactions [like those at location $(-1, -1)$ in Fig. 2a.1]. The forces associated with the other regions would either repel [like those at location (0,0) in Fig. 2a.1] or be too weak to attract [like those at location $(-1,0)$ and $(0, -1)$ in Fig. 2a.1] the large paramagnetic particle.

The effect of the magnetite particle separation s on the z-component of the interaction force between the array and two different-sized paramagnetic particles with radii of 160 and 1000 nm is shown in Figs. 3 and 4 in terms of the x and y coordinates and for $h = 20$ nm and $\alpha = 90^\circ$. Figs. 3a.1 to 3a.3 and Figs. 4a.1 to 4a.3 are for $r_p = 160$ nm, and Figs. 3b.1 to 3b.3 and Figs. 4a.1 to 4a.3 are for $r_p = 1000$ nm. Figs. 3 and 4 combined show the sequential change of the profiles of the magnetic force within the square defined in Fig. 1b as the magnetite particle separation is varied from $s = 1$ (Figs. 3a.1 and 3b.1) to $s = 0$ (Figs. 4a.3 and 4b.3) in increments of 0.2. For the smaller paramagnetic particle, as s decreases, the interaction between the paramagnetic particle and the array varies from one where the paramagnetic particle individually interacts with only a single magnetite particle ($s = 1.0$) to one where the strong and cooperative lateral interactions caused by the closer proximity of the paramagnetic particle to several other magnetite particles in the array become apparent ($s = 0.0$). One consequence of this cooperative effect is the appearance of a repulsive region centered around location (0,0) that increases with decreasing s, as clearly noticed in Figs. 4a.1, 4a.2, and 4a.3. In contrast, for larger s, the profiles in Figs. 3a.1, 3a.2, and 3a.3 ($s = 1.0$, 0.8, and 0.6, respectively) simply exhibit relatively flat zones, except near the corners, which is indicative of the paramagnetic particle interacting with only a single magnetite particle.[5] This cooperative effect is also responsible for the monotonous decrease of the attractive interaction experienced by the paramagnetic particle at each corner of the figure

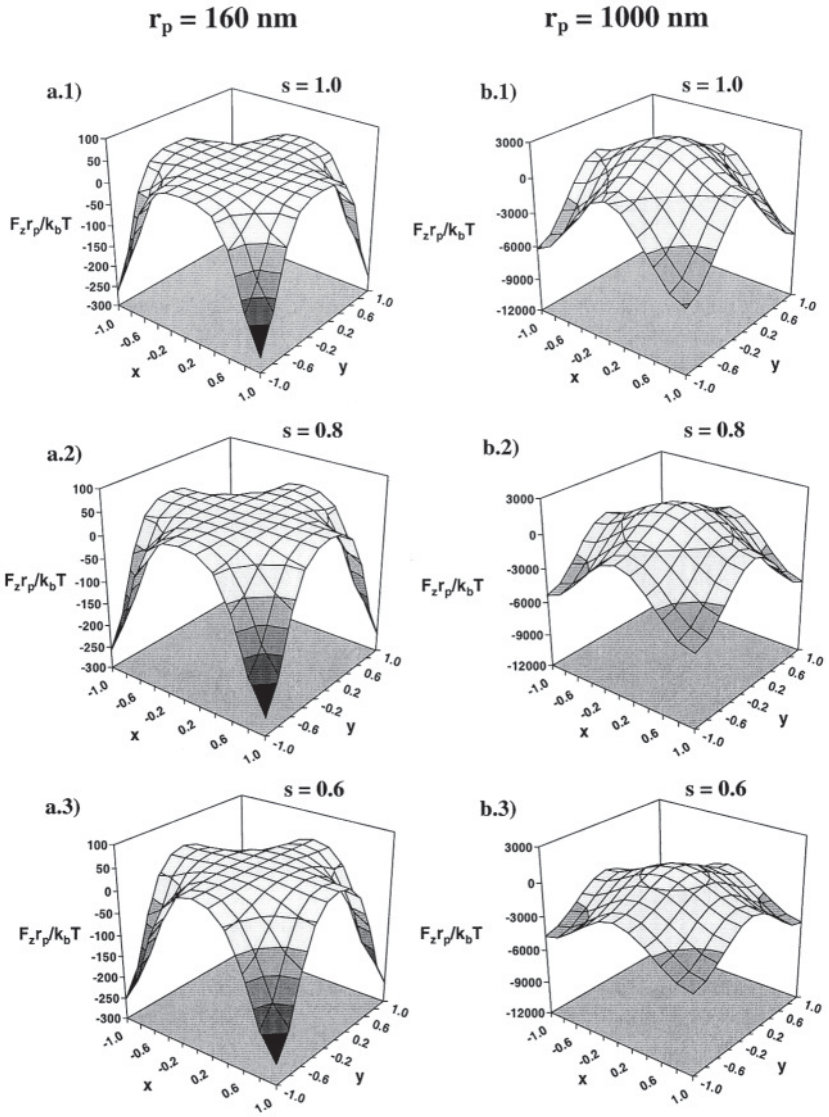

Figure 3. z-Component of the total magnetic force exerted by the array of magnetite particles on the paramagnetic particle with radius r_p equal to a) 160 nm and b) 1000 nm within the square defined in Fig. 1b for $\alpha = 90^\circ$, $h = 20$ nm and a) $s = 1.0$, b) s = 0.8 and c) s = 0.6. All other parameters are fixed and given in Table 1.

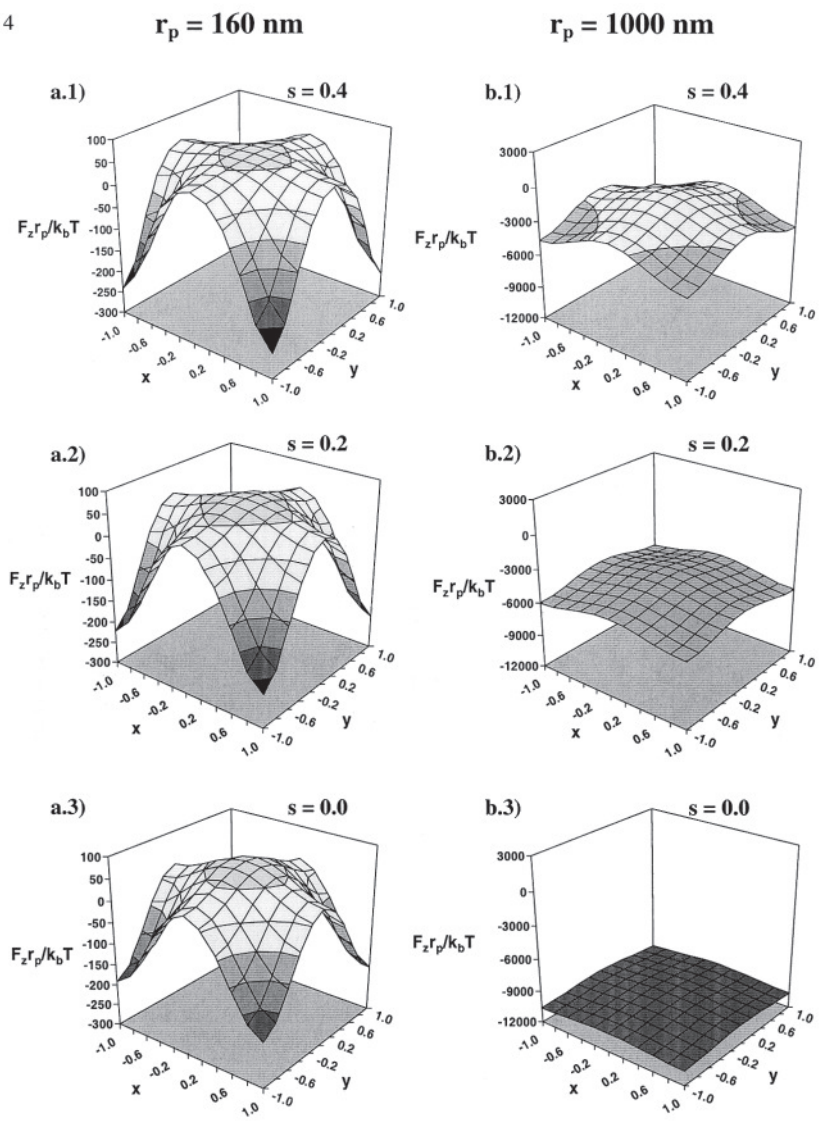

Figure 4. z-Component of the total magnetic force exerted by the array of magnetite particles on the paramagnetic particle with radius r_p equal to a) 160 nm and b) 1000 nm within the square defined in Fig. 1b for $\alpha = 90^\circ$, $h = 20$ nm and a) $s = 0.4$, b) $s = 0.2$ and c) $s = 0.0$. All other parameters are fixed and given in Table 1.

where the center of a magnetite particle is located [i.e., at $(-1.0, -1.0)$, $(-1.0,1.0)$, $(1.0, -1.0)$, and $(1.0,1.0)$]. This attractive interaction decreases from a dimensionless value of around 255 at $s = 1.0$ (Fig. 3a.1) to a value around 185 at $s = 0.0$ (Fig. 4a.3). The corresponding interaction between only a single magnetite particle and the paramagnetic particle would be essentially the same as that for the case with $s = 1.0$ (Fig. 3a.1).[5] Hence, the monotonous decrease in the interaction is clearly due to the presence of the other magnetite particles in the array. The trends exhibited by the large paramagnetic particle are distinctly different, however.

First, notice that the profile of the z-component of the force on the large paramagnetic particle with $s = 1.0$ (Fig. 3b.1) is very similar to that exhibited by the small paramagnetic particle with $s = 0.0$ (Fig. 4a.3), indicating that the large paramagnetic particle senses the lateral interactions even at large separations s between the magnetite particles. It is surmized that this situation would persist for the large paramagnetic particle even for $s \gg 1.0$, simply because the size of the large paramagnetic particle is on the order of the size of the array itself. Also, unlike the monotonically decreasing interaction with the smaller paramagnetic particle, the interaction with the larger paramagnetic particle at the locations of the magnetite particles [i.e., at $(-1.0, -1.0)$, $(-1.0,1.0)$, $(1.0, -1.0)$, and $(1.0,1.0)$] at first decreases with decreasing s, reaches a minimum at about $s = 0.4$ (in this particular case), and then increases again as s decreases to 0.0. For example, the dimensionless value of the force at $(-1.0, -1.0)$ decreases from a value of around 5800 at $s = 1.0$ (Fig. 3b.1) to a value of around 4600 at $s = 0.4$ (Fig. 4b.1) and then increases to a value of around 10500 at $s = 0.0$ (Fig. 4b.3). It is also interesting to point out that for this particular situation the profiles become considerably flatter with decreasing s. As explained earlier, this situation results from the fact that the array begins to interact with the large paramagnetic particle as one large magnetic unit, which causes the z component of the force to become not only larger but also "smoother" across the surface with decreasing s.

As pointed out from the results shown in Fig. 2, the behavior of the array as a single magnetic unit is observed not only at small magnetite particle separations s, but also at large distances h between the array and the paramagnetic particle, which occurs at $h > 600$ nm for the results shown in Fig. 2. The effect of s was further revealed for both the small and large paramagnetic particles from the results shown in Figs. 3 and 4. Now, the results shown in Fig. 5 further reveal the effect of h, again in terms of the interaction force profiles as a function of the x and y coordinates for six different values of h sequentially varying from 20 nm (Fig. 5a) to 1000 nm (Fig. 5f), and for $r_p = 1000$ nm, $s = 1.0$ and $\alpha = 90^\circ$. It is intriguing how the "roughness" (manifested by the marked spatially dependent repulsive and attractive

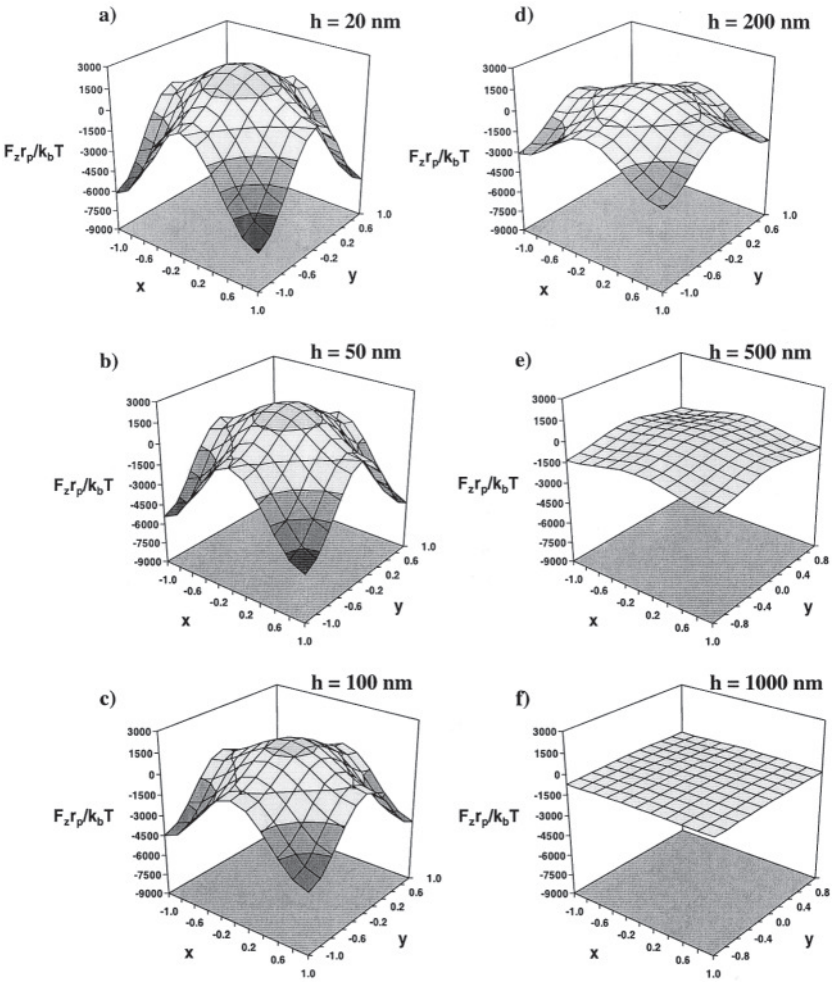

Figure 5. z-Component of the total magnetic force exerted by the array of magnetite particles on the paramagnetic particle with radius r_p equal to 1000 nm within the square defined in Fig. 1b for $\alpha = 90$, $s = 1.0$ and a) $h = 20$ nm, b) $h = 50$ nm, c) $h = 100$ nm, d) $h = 200$ nm, e) $h = 500$ nm, and f) $h = 1000$ nm. All other parameters are fixed and given in Table 1.

zones) observed at $h = 20$ nm for the dimensionless z component of the force (Fig. 5a) slowly vanishes with increasing h, essentially becoming very attractive (dimensionless force of around -700) and flat (or "smooth") at $h = 1000$ nm (Fig. 5f). This relatively large and spatially independent

constant value of the dimensionless force at about -700 clearly shows that the interactions observed at this large h cannot be attributed to the individual interactions exerted by the magnetite particles on the paramagnetic particle. Instead, the only plausible way to explain this behavior is to attribute the interaction exerted on the paramagnetic particle to the entire array acting as a single magnetic unit. It is also remarkable that the effect of the magnetite particles in the array behaving either collectively as a single magnetic unit at large h or individually with nearest neighbors each providing their own cooperative interaction at small h is still observed at magnetite particle separations as great as one magnetite particle diameter (i.e., $s = 1.0$). This multifunctional behavior manifests in this case simply because the size of the paramagnetic particle is on the order of the size of the array.

Another unique characteristic associated with the behavior of the array that is clearly depicted in Fig. 5 is the substantial changes exhibited by the force at different distances h between the array and the paramagnetic particle. Notice, for example, that the repulsive force observed at around location (0,0) not only decreases with larger h, but also becomes attractive when h becomes larger than 500 nm. This result further substantiates the existence of two types of regions that dictate the interactions between the array and the paramagnetic particle: one where the net force is dominated by short-ranged forces originating from the individual magnetite particles, and the other one where the net force is absolutely dominated by long-ranged forces originating from the array behaving collectively as one large magnetic unit.

Figure 6 provides a summary of all the results discussed in terms of h/r_m vs. s parameter space. Qualitatively, this figure shows the conditions for which the interaction between the array and a paramagnetic particle is either due to the particles in the array behaving collectively as one large magnetic unit or individually with cooperative nearest neighbor effects. Two situations are analyzed. Figure 6a depicts the case where the paramagnetic particle is smaller than the magnetite particles in the array (i.e., $r_p/r_m < 1.0$), which qualitatively summarizes the results given elsewhere[5] and in Figs. 3b and 4b. Figure 6b depicts the case where the paramagnetic particle is larger than the magnetite particles in the array (i.e., $r_p/r_m > 1.0$), which qualitatively summarizes the results in Figs. 2, 3a, 4a, and 5. The regions for which the array behaves mainly as a single magnetic unit are represented in dark gray and labeled as "collective." The regions for which the particles in the array each interact individually with the paramagnetic particle in a cooperative manner are represented in light gray and labeled "individual." The overlapping regions for which both types of interactions play significant roles are represented in light gray with diagonal lines.

For small paramagnetic particles ($r_p/r_m < 1.0$, Fig. 6a) the strictly collective region is small and only comes into play for distances h between

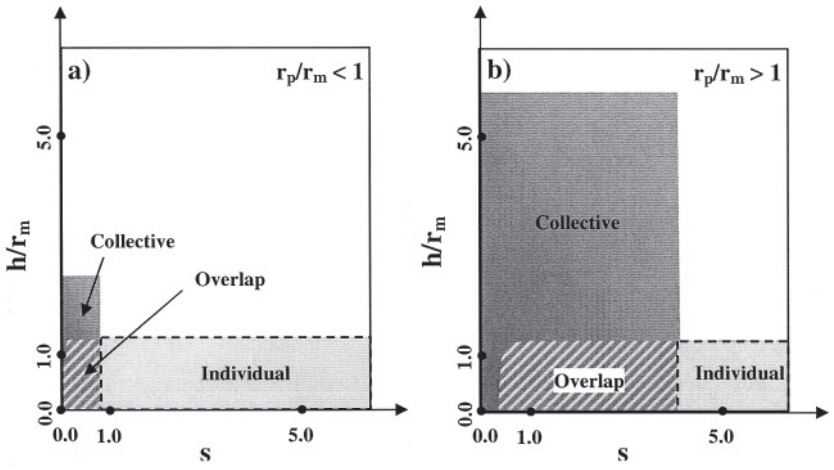

Figure 6. Plot of parameter space h/r_m as a function of s map that qualitatively defines the conditions for which different types of interactions that take place between an array of magnetite particles and a paramagnetic particle that is a) smaller and b) larger than the magnetite particles in the array. The regions for which the array behaves mainly as a single magnetic unit are represented in dark gray and labeled as "collective." The regions for which the particles in the array each interact individually with the paramagnetic particle in a cooperative manner are represented in light gray and labeled "individual." The overlapping regions for which both types of interactions play significant roles are represented in light gray with diagonal lines and labeled "overlap."

the paramagnetic particle and the array that are greater than r_m and for separations s between the magnetite particles that are less than one. The corresponding interactions are relatively short-ranged and cease to exist at h/r_m values greater than about two. In contrast, the strictly individual region is quite broad and persists alone at essentially any value of $s > 1.0$; however, again the corresponding interactions are extremely short-ranged and cease to exist at h/r_m values greater than about one. The overlapping region where both collective and individual interactions occur are bounded by h/r_m and s both being less than one. For large paramagnetic particles ($r_p/r_m > 1.0$, Fig. 6b), the strictly collective region is quite large and comes into play not only for $h \gg r_m$, but also for values of h/r_m approaching zero but only for very small values of s also approaching zero. For values of $h/r_m > 1.0$, the collective region persists for relatively large values of s, which is distinctly different from that exhibited by small paramagnetic particles. This trend indicates that for particularly small values

of *s*, the array is capable of interacting as a single magnetic unit, but only with a paramagnetic particle that is much larger than a magnetite particle (Fig. 6b). This behavior is observed in Figs. 2a.3, 2b.3, 4b.2, and 4b.3, and due to the fact that the individual interactions between the paramagnetic particle and the magnetite particles become less lateral and more vertical as *s* becomes smaller. In contrast, a paramagnetic particle that is much smaller than a magnetite particle is not capable of experiencing this interaction, even when the magnetite particles are in contact with each other, i.e., with $s = 0.0$ (Fig. 6b; also see Fig. 4a.3). In this case, the gradients associated with the entire array are so small that the forces on the small paramagnetic particle are overwhelmed by the short-ranged interactions caused by the individual magnetite particles in the array, especially those in close proximity to the paramagnetic particle. The corresponding interactions with the large paramagnetic particles compared with the small paramagnetic particles in the strictly collective region are also distinctly different, being very long-ranged over broad ranges of h/r_m and *s*. In contrast, the strictly individual region is quite narrow and persists alone at essentially any value of $s \gg 1.0$; however, again the corresponding interactions are extremely short-ranged and cease to exist as h/r_m values greater than one. The overlapping regions where both collective and individual interactions occur are still bounded by h/r_m being less than one, but not *s*. For large paramagnetic particles, the overlapping region comes into play at relatively small values of *s* and persists up to moderately large values of *s* because the collective region is quite broad.

The multifunctional character of a magnetite particle cluster was manifested by its ability to impart interactions collectively as a single magnetic unit or through interactions with individual magnetite particles in the array, or even to impart both interactions simultaneously. This multifunctional behavior of a magnetite cluster clearly stems from its ability to exert distinctly different forces or interactions on small paramagnetic particles compared to large paramagnetic particles. And, of course, this behavior depends markedly on the separation *s* between the magnetite particles and the distance *h* between the array and the paramagnetic particle, as revealed qualitatively in Fig. 6, and quantitatively in Figs. 2 to 5 and in previous work.[5] Moreover, for both situations depicted in Figs. 6a and 6b there is a distance *h* where the short-ranged interactions either cease to exist or transform into long-ranged interactions created by the array as a whole for any value *s*. In general, this particular *h* seems to be a very weak function of the size of the paramagnetic particle (r_p). For example, it turns out to be around 600 nm (see Figs. 2, 5e, and 5f) for the particular system and conditions studied here, which is nearly identical to that reported in the previous work[5] under identical conditions but for much smaller paramagnetic particles.

CONCLUSIONS

The magnetic force exerted by a $10 \times 10 \times 5$, 3-D array of identically sized magnetite particles ($r_m = 400$ nm) on two differently sized paramagnetic particles ($r_p = 160$ and 1000 nm) was investigated to extend previous work by the authors to the case where the paramagnetic particles were much larger than a single magnetite particle approaching the size of the array itself, and then to confirm previous speculations about the multifunctional character of magnetite particle clusters and their ability to magnetically retain a wide range of sizes of weakly paramagnetic particles. In this study, the size of the smaller paramagnetic particle ($r_p = 160$ nm) was purposely chosen to be close to the size of a single magnetite particle in the array, where as the larger one ($r_p = 1000$ nm) was purposely chosen to be close to the size of the array itself. Three important parameters were studied: the orientation α of the magnetic field, the separation s between the magnetite particles in the array, and the normal distance h between the paramagnetic particle and the surface of the array.

The orientation α of the magnetic field simply produced maximum and bounding interactions at orthogonal conditions, with the resulting repulsive interactions at $\alpha = 0^\circ$ (with H_a parallel to the surface of the array) always being less than the resulting attractive interactions at $\alpha = 90^\circ$ (with H_a perpendicular to the surface of the array). This result has interesting implications with respect to the use of supported magnetic particle clusters as a HGMS element. Since on average α is expected to be about 45° for magnetic particle clusters with randomly distributed surfaces, the magnitude of the interaction force will never be greater than that observed and bounded by the orthogonal orientations of the magnetic field at $\alpha = 0$ and 90°. The direction of the interaction force (i.e., whether the force is attractive or repulsive), on the other hand, will tend to be attractive because the magnitude of the attractive force (with $\alpha = 90^\circ$) was always observed to be greater than the magnitude of the repulsive force (with $\alpha = 0^\circ$) under the same conditions.

The effects of both s and h on the magnitude of the interaction force between the paramagnetic particle and the array were quite pronounced and depended noticeably on the size of the paramagnetic particle. Both the large and small paramagnetic particles experienced interactions with the array that were strictly due to the array behaving collectively as a single magnetic unit; but, these relatively "smooth" interactions were much longer-ranged for the large paramagnetic particle. The large and small paramagnetic particles also experienced interactions with the array that were strictly due to individual (yet cooperative) interactions with each of the magnetite particles in the array, especially those in close proximity to the paramagnetic particle; but, in most cases, these individual and relatively "rough" interactions were short-ranged

for both paramagnetic particles. Not only did the spatial range of these solitary (multifunctional) interactions depend markedly on the values of h and s, and especially r_p, but so did the spatial range of the regions where these collective and individual interactions overlapped, which was much bigger for the larger paramagnetic particle simply because the collective region was much bigger. The long-ranged and very "smooth" interactions were caused by the entire array interacting with a paramagnetic particle as a single magnetic unit, whereas the short-ranged and relatively "rough" interactions were caused by the magnetite particles in the array individually interacting in a cooperative manner. Clearly, the multifunctional character of the magnetite particle cluster was manifested by its ability to impart interactions collectively as a single magnetic unit or through individual (yet cooperative) magnetite particles in the array, or even to impart both interactions simultaneously, with all three situations depending on the conditions.

Overall, as a HGMS element, this unique multifunctional character of magnetite particle clusters could give various forms of supported magnetite a key advantage over traditional stainless steel wool for retaining both large and especially small paramagnetic particles of weak magnetic character. A supported magnetite element should be able to attract paramagnetic particles of weak magnetic character ranging in size from a small magnetite particle to the entire array (i.e., a magnetite particle cluster). In general, a traditional stainless steel wool HGMS element would have difficulty retaining the small paramagnetic particles on the order of the size of a magnetite particle. It is fortuitous that supporting theoretical and experimental evidence of this unique ability of magnetite particle clusters to exhibit multifunctional character is beginning to appear in the literature.

NOMENCLATURE

$F^*_{m,i}$	j-coordinate of the dimensionless magnetic force between the paramagnetic particle and the array of magnetite particles applied to the system of coordinates x, y and z, N
$F_{m,i}$	j-coordinate of the magnetic force between the paramagnetic particle and the array of magnetite particles applied to the system of coordinates x, y and z, N
$F_{m,i,j}$	j-coordinate of the magnetic force between the paramagnetic particle and magnetite particle i applied to any system of coordinates, N
$F_{m,r}$	radial component of the magnetic force between a magnetite particle and a paramagnetic particle with the origin at the center of the magnetite particle, N

$F_{m,\theta}$	angular component of the magnetic force between a magnetite particle and a paramagnetic particle with the origin at the center of the magnetite particle, N
G	constant defined in Eq. (3c)
h	surface-to-surface distance between the paramagnetic particle and the plane that is tangent to the top layer of the magnetite particles in the array and parallel to the x-y plane, m
H_a	scalar form of the externally applied magnetic field, A m^{-1}
k_b	Boltzmann constant, 1.3807×10^{-23} J K^{-1}
k_i	index corresponding to magnetite particle i in the x-direction
l_i	index corresponding to magnetite particle i in the y-direction
m_i	index corresponding to magnetite particle i in the z-direction
M_s	saturation magnetization of magnetite, A m^{-1}
N	number of magnetite particles in the array
r	center-to-center distance between a paramagnetic particle and a magnetite particle; radial coordinate in the spherical coordinate system, m
r_m	radius of a magnetite particle, m
r_p	radius of a paramagnetic particle, m
s	ratio of the surface-to-surface separation between the magnetite particles in the array and their diameter
T	temperature, K
V_p	volume of the paramagnetic particle, m^3
x	dimensionless form of X_p^* according to Eq. (14a)
X_i^*	x-coordinate of the paramagnetic particle relative to the center of magnetite particle i, m
$X_{m,i}$	x-coordinate of magnetite particle i with respect to the origin defined in Fig. 2b, m
X_p	x-coordinate of the paramagnetic particle with respect to the origin defined in Fig. 2b, m
y	dimensionless form of Y_p^* according to Eq. (14b)
Y_i^*	y-coordinate of the paramagnetic particle relative to the center of magnetite particle i, m
$Y_{m,i}$	y-coordinate of the magnetite particle i with respect to the origin defined in Fig. 2b, m
Y_p	y-coordinate of the paramagnetic particle with respect to the origin defined in Fig. 2b, m
Z_i^*	z-coordinate of the paramagnetic particle relative to the center of magnetite particle i, m
$Z_{m,i}$	z-coordinate of the magnetite particle i with respect to the origin defined in Fig. 2b, m

Z_p z-coordinate of the paramagnetic particle with respect to the origin defined in Fig. 2b, m

Greek Symbols

α angle between the y-axis and the applied magnetic field H_a in the plane parallel to the z-y plane, as depicted Fig. 1
χ_m volumetric magnetic susceptibility of the medium
χ_p volumetric magnetic susceptibility of the paramagnetic particle
ϕ_i azimuthal angular coordinate in the spherical coordinate system defined in Fig. 4, with the origin at the center of magnetite particle i
μ_o magnetic permeability of free space, $4\pi \times 10^{-7}$, $\mathrm{T\,m\,A^{-1}}$
μ_m magnetic moment of magnetite, $\mathrm{A\,m^2}$
θ polar angular coordinate in the spherical coordinate system
θ_i polar angular coordinate in the spherical coordinate system defined in Fig. 4, with the origin at the center of magnetite particle i

ACKNOWLEDGMENT

The authors gratefully acknowledge financial support from the National Science Foundation under Grant No. CTS-9985489.

REFERENCES

1. Kochen, R.L.; Navaratil, J.D. Removal of radioactive materials and heavy metals from water using magnetic resin. U.S. Patent 5,595,666, 1997.
2. Ebner, A.D.; Ritter, J.A.; Ploehn, H.J. Feasibility and limitations of nano-level high gradient magnetic separation. Sep. Purif. Technol. **1997**, *11*, 199–210.
3. Ebner, A.D.; Ritter, J.A.; Ploehn, H.J.; Kochen, R.L.; Navratil, J.D. New magnetic field-enhanced process for the treatment of aqueous wastes. Sep. Sci. Technol. **1999**, *34*, 1277.
4. Ebner, A.D.; Ritter, J.A.; Ploehn, H.J. Magnetic hetero-flocculation of paramagnetic colloidal particles. J. Colloid. Interf. Sci. **2000**, *225*, 39.
5. Ebner, A.D.; Ritter, J.A.; Ploehn, H.J. Magnetic field orientation and spatial effects on the retention of paramagnetic nanoparticles with magnetite. Sep. Sci. Tech. **2002**, *37*, 3727–3753.
6. Eisenstein, I. Magnetic separators: Traction force between ferromagnetic and paramagnetic spheres. IEEE Trans. Magn. **1977**, *13*, 1646.

7. Badescu, V.; Rotariu, O.; Murariu, V.; Rezlescu, N. Transverse high gradient magnetic filter with bounded flow field. IEEE Trans. Magn. **1997**, *33*, 4439.
8. Hayashi, E.; Uchiyama, S. On the trajectory and capture efficiency around many wires. IEEE Trans. Magn. **1980**, *16*, 827.
9. Eisenstein, I. Magnetic traction force in an HGMS with an ordered array of wires: II. IEEE Trans. Magn. **1978**, *14*, 1155.
10. Eisenstein, I. Magnetic traction force in an HGMS with an ordered array of wires: I. IEEE Trans. Magn. **1978**, *14*, 1148.
11. Shen, J.C.; Ebner, A.D.; Ritter, J.A. Points of zero charge and intrinsic equilibrium constants of silica-magnetite composite oxides. J. Colloid. Interf. Sci. **1999**, *214*, 333.